



HAL
open science

Experimental study and modelling heat transfer during condensation of pure fluid and binary mixtures on a bundle of finned tubes

Mourad Belghazi, André Bontemps, Christophe Marvillet

► **To cite this version:**

Mourad Belghazi, André Bontemps, Christophe Marvillet. Experimental study and modelling heat transfer during condensation of pure fluid and binary mixtures on a bundle of finned tubes. International Journal of Refrigeration, 2003, 26 (2), pp.214-223. 10.1016/S0140-7007(02)00042-7 . hal-00184124

HAL Id: hal-00184124

<https://hal.science/hal-00184124>

Submitted on 11 Feb 2020

HAL is a multi-disciplinary open access archive for the deposit and dissemination of scientific research documents, whether they are published or not. The documents may come from teaching and research institutions in France or abroad, or from public or private research centers.

L'archive ouverte pluridisciplinaire **HAL**, est destinée au dépôt et à la diffusion de documents scientifiques de niveau recherche, publiés ou non, émanant des établissements d'enseignement et de recherche français ou étrangers, des laboratoires publics ou privés.



Distributed under a Creative Commons Attribution 4.0 International License

Experimental study and modelling of heat transfer during condensation of pure fluid and binary mixture on a bundle of horizontal finned tubes

M. Belghazi^a, A. Bontemps^{b,*}, C. Marvillet^{a,1}

^a*Groupement pour la Recherche sur les Echangeurs thermiques (GRETh),
Commissariat à l'Energie Atomique, 17, rue des Martyrs, 38054 Grenoble Cedex 9, France*

^b*LEGI/GRETh, Université Joseph Fourier, Grenoble, France*

An experimental investigation was conducted to measure the local heat transfer coefficient for each row in a trapezoidal finned horizontal tube bundle during condensation of both pure fluid (HFC 134a) and several compositions of the non-azeotropic binary mixture HFC 23/HFC 134a. The test section is a 13×3 (rows × columns) tube bundle and the heat transfer coefficient is measured using the modified Wilson plot method. The inlet vapour temperature is fixed at 40 °C and the water flow rate in each active row ranges from 170 to 600 l/h. The test series cover five different finned tubes all commercially available, K11 (11 fins/inch), K19 (19 fins/inch), K26 (26 fins/inch), K32 (32 fins/inch), K40 (40 fins/inch) and their performances were compared. The experimental results were checked against available models predicting the heat transfer coefficient during condensation of pure fluids on banks of finned tubes. Modelling of heat exchange during condensation of binary mixtures on bundles of finned tubes based on the curve condensation model is presented.

Keywords: Heat transfer; Mass transfer; Condensation; Refrigerant; Binary mixture; Finned tube; Exterior; Bundle; Heat transfer coefficient; Measurement; Modelling

* Corresponding author. Tel.: +33-4-3878-3155; fax: +33-4-3878-5172.

E-mail address: andre.bontemps@ujf-grenoble.fr (A. Bontemps).

Nomenclature

a	thermal diffusivity ($\text{m}^2 \text{s}^{-1}$)
A	ratio of the total to the plain tube surfaces
b	fin spacing (m)
C_p	specific heat capacity ($\text{J kg}^{-1} \text{K}^{-1}$)
$D_{1,2}$	mass diffusivity ($\text{m}^2 \text{s}^{-1}$)
D_e	diameter at the fin tip (m)
D_h	hydraulic diameter (m)
D_i	inner diameter (m)
D_r	Diameter at the fin root (m)
e	fin height (m)
F	correction factor
g	gravity (m s^{-2})
h_m	specific enthalpy (J kg^{-1})
j	row index
K	constant
\dot{m}	mass flow rate (kg s^{-1})
N	row number
p	fin pitch (m)
P	pressure (N m^{-2})
q	heat flux (W m^{-2})
Q	heat flow rate (W)
S	exchange surface area (m^2)
t	fin thickness (m)
T	temperature (K)
U	overall heat transfer coefficient ($\text{W m}^{-2} \text{K}^{-1}$)
v	vapour velocity (m s^{-1})
x_g	vapour quality
y	HFC23 mass fraction
Z	Bell and Ghaly parameter
\dot{Z}	modified Bell and Ghaly parameter

Greek letters

α_{avg}	vapour phase mean heat transfer coefficient in the bundle ($\text{W m}^{-2} \text{K}^{-1}$)
α_e	vapour-side heat transfer coefficient ($\text{W m}^{-2} \text{K}^{-1}$)
α_i	inner heat transfer coefficient ($\text{W m}^{-2} \text{K}^{-1}$)
α_l	heat transfer coefficient in the liquid phase ($\text{W m}^{-2} \text{K}^{-1}$)
α_v	local heat transfer coefficient in the vapour phase ($\text{W m}^{-2} \text{K}^{-1}$)
β	inundation coefficient
ϵ	enhancement factor
λ	thermal conductivity ($\text{W m}^{-1} \text{K}^{-1}$)
Φ	flooding angle (rad)
θ	half angle at the fin tip (rad or degree)
σ	surface tension (N m^{-1})

Subscripts

c	coolant
g	gas
G	Gnielinski
in	inlet
j	row index
l	liquid
out	outlet
T	total
v	vapour
w	wall

Dimensionless numbers

Le	Lewis number
Nu	Nusselt number
Pr	Prandtl number
Re	Reynolds number

1. Introduction

In the European context where existing and new refrigerating machines have to be adapted to HFCs (HydroFluoroCarbons), the questions asked of heat exchanger designers and thermal engineers generally fall into two groups. The first concerns the behaviour of traditionally designed TEMA X¹ condensers which have to operate with retrofitting refrigerants especially with zeotropic mixtures. The second covers the optimisation of the TEMA X condenser to pure HFCs as HFC 134a and to mixed refrigerants (e.g. HFC 407C).

To answer the both items, the present study, which expands on a preliminary study on smooth tube bundles [1], deals with the experimental evaluation of heat transfer performance of tube bundles equipped with finned tubes whose density ranges from 11 to 40 fpi.

The present work has four aims: (i) to study condensation outside five different finned tubes in order

to underline the influence of the fin pitch, (ii) to study condensation of several compositions of the binary mixture (HFC 23/HFC 134a), (iii) to understand heat transfer in enhanced tube banks both with pure fluids and with mixtures, and (iv) to model heat transfer in tube bundles during condensation of zeotropic mixtures by means of the equilibrium method.

2. A short review of relevant works

2.1. Pure fluid case

Theoretical models to predict the heat transfer coefficient (HTC) for single low-finned tubes have been well developed since the 1940's, in particular with the pioneering work of Beatty and Katz [2]. Their model assumed that the condensate is drained only via gravity. Gregorig [3] was the first author to develop a model of condensation around profiled surfaces, taking into

account only the surface tension forces. A review of surface tension effects during condensation of pure fluids is given by Shah et al. [4].

Theoretical models combining both gravity and surface tension forces are used to predict the HTC of a single horizontal tube with sufficient accuracy. Rose [5] proposed a semi-empirical model for a horizontal tube having trapezoidal fins. To compare his model to experimental results, Rose [5] used various finned tubes with different fin pitches, heights and diameters as well as various fluids (water, ethylene glycol, methanol, R113, R11, R12...). He found a deviation of 12.4% from the experimental data used.

The foregoing models for a single tube are not directly applicable to tube banks, since heat transfer in the lower rows is affected by condensate inundation and the HTC is lower for these tubes. In the literature there are two approaches to this problem. The first simply consists of multiplication of the HTC for a single tube by a factor less than unity, taking into account the row position in the bundle. The second, more accurate, consists in the development of a model, first for a single tube, and then for a bundle. Such a model was proposed by Honda and Nozu [6,7] based on a bidimensional analysis of the film condensate. Murata and Hashizume [8] developed a model predicting the HTC of tube bundles having rectangular fins. To validate their model they compared it to experimental data during condensation of R11 and R114 in bundles of eight rows, with rectangular fin tubes of various fin pitches. Theory and experiments differed by about 20%.

There are few experiments on the condensation of HFC134a on low finned tubes. In the work of Blanc [9], the HTC on trapezoidal fin tubes (K26) is compared with current theories. In particular, the Honda model underestimates by up to -30% the inundation effect of their experimental results.

Honda et al. [10] measured the row-by-row HTCs of HFC134a condensing on a bundle of tubes having 26 fins/inch and a diameter at the fin root of 15.8 mm. Their results are slightly lower than those of Blanc. Cheng and Wang [11] and Ravi et al. [12] conducted experiments on condensation of HFC134a using several types of low finned tubes. The former found that for a vertical column of three tubes with trapezoidal fins no significant inundation effect is observed. The latter studied the HTC variation as a function of ΔT for a single tube.

2.2. Fluid mixture case

In contrast to the pure fluid, the condensation of zeotropic mixtures outside enhanced horizontal tubes has been not widely investigated. Studies covering the condensation of zeotropic mixtures are essentially confined to flat plates and smooth tubes. Hijikata and Himeno [13] conducted experiments using horizontal

finned tubes during condensation of the binary mixture (90% R113 + 10% R114) and they found that the tube with high fins (3 mm) is better than the one with small fins (0.8 mm), contrary to the condensation of pure fluids. Honda et al. [14] conducted experiments during condensation of a downward-flowing zeotropic mixture HFC123/HFC134a (about 9% HFC134a at the test section inlet), on a 13 × 15 (columns × rows) staggered bundle of horizontal low finned tubes. Their experimental data show that both the heat and mass transfer coefficients increase with the row number up to the third (or the second) row, then decrease monotonically with increasing row number, finally to increase at the last row. To correlate their results they proposed a dimensionless correlation of the mass transfer coefficient based on the analogy between heat and mass transfer.

3. Experimental apparatus

The experimental apparatus consists of a thermosiphon refrigerant loop and a forced circulation coolant (water) loop (Fig. 1). The test rig used in this investigation is the same as that of a previous study [1]. In the refrigerant loop the vapour is generated in a boiler heated with hot water which is itself heated by an electric heater. The vapour flows towards the test section, passes vertically downwards and condenses outside the water cooled tubes. The test section (Fig. 2) is a stainless steel duct and contains a staggered copper tube bank consisting of 13 rows, each of two (even rows) or three tubes (odd rows). In Fig. 2 the cross-hatched tubes are dummies (no heat exchange), while the others are active. Half tubes are attached to the vertical walls of the test section in order to eliminate vapour by-pass. A metallic rod with a diameter of 11 mm was inserted in each active tube in order to increase the water velocity. In this way the heat transfer is enhanced on the coolant side. The horizontal tube pitch is 24 mm, whereas the vertical pitch is 20 mm. The tube length is 300 mm. The characteristics of the tested tubes are given in Table 1. The vapour temperature inlet was maintained at 40 °C and the vapour velocity is less than 2 m/s. Temperatures were measured by type E thermocouples (Chromel-Constantan) with a precision of ± 0.1 K. As water flow is equally distributed in all active tubes (it is controlled by means of 13 rotameters, one on each row), the water flow rate in each tube is deduced from the water flow rate in the coolant loop, measured by an electromagnetic flow meter, with an accuracy of $\pm 0.5\%$. The vapour temperature is measured using five thermocouples (T06, T07, T08, T09 and T10) in the test section. The temperatures indicated by the five thermocouples are interpolated in order to obtain the vapour temperature in the neighbourhood of each row.

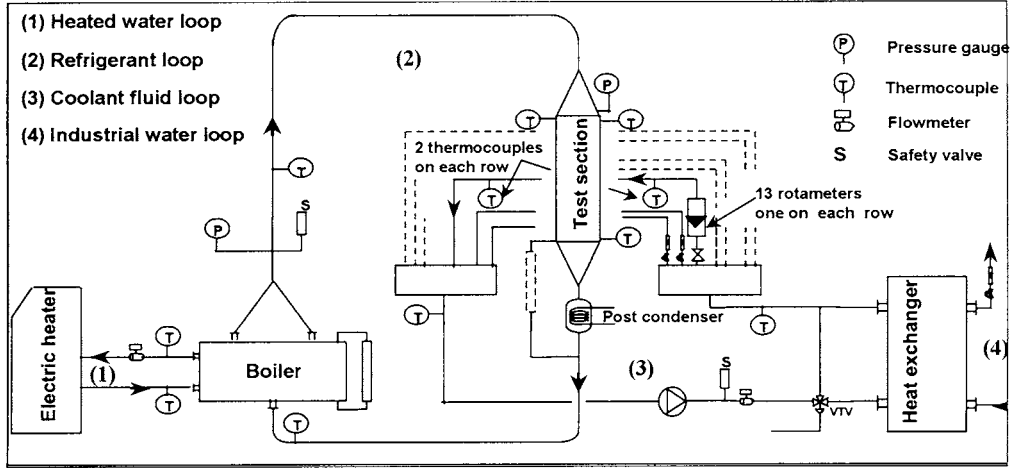


Fig. 1. Experimental test rig.

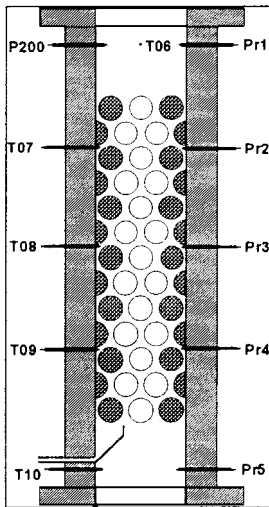


Fig. 2. Test section.

Table 1
Tube dimensions

Tube	D_r (mm)	D_e (mm)	D_i (mm)	p (mm)	e (mm)	t (mm)	A	θ (degree)
K11	16	18.9	14	2.31	1.45	0.38	2.4	1
K19	16	18.9	14	1.34	1.45	0.33	3.4	1.9
K26	15.8	18.8	14	0.97	1.5	0.25	4.4	3.5
K32	16.2	18.8	14	0.82	1.3	0.2	4.5	?
K40	16.3	18.9	14.4	0.63	1.3	0.16	5.5	?

In this study, commercially available tubes (Wieland-Werke AG) are used, having a wall thickness of about 1 mm, and the indirect Wilson method which measures the vapour-side HTC without measuring the wall temperature is employed. From the measured water temperatures at the inlet and the outlet of each tube and from the mea-

sured vapour temperature in the neighbourhood of each row, the overall HTC is calculated as follows:

$$U = \frac{\dot{m}_c C_{p,c}}{S} \ln \left(\frac{T_{v,j} - T_{c,in}}{T_{v,j} - T_{c,out}} \right) \quad (1)$$

The vapour-side HTC α_e is calculated by the following relation:

$$\frac{1}{\alpha_e} = \frac{1}{U} - \frac{1}{\alpha_i} \frac{D_r}{D_i} - \frac{D_r}{2\lambda_w} \ln \left(\frac{D_r}{D_i} \right) \quad (2)$$

α_i is the inner HTC determined with Eq. (3) using the Gnielinski correlation [15] to determine the Nusselt number Nu_G . The Gnielinski correlation was chosen because it has a wide range of applicability, $2300 < Re_c < 5 \cdot 10^6$ and $0.5 < Pr < 2000$. Thus, it covers both the transition and the turbulent flow regimes. In the present case, the Reynolds number varied between 2400 and 10 000:

$$\alpha_i = K \cdot Nu_G \cdot \frac{\lambda_c}{D_h} \quad (3)$$

K is determined by the modified Wilson plot procedure [16]. This procedure requires the use of a water-water counter current single phase heat exchanger in which the inner tube is the same as in the test section.

The overall HTC U has a relative uncertainty of 14.8%, and the calibration of the inner HTC of K11, K19, K26, K32 and K40 tubes leads respectively to relative uncertainties of 10.3, 8.9, 5.4, 13.4 and 4.5%, all determined using Moffat's method of sequential disturbances [17]. The relative uncertainty of the vapour-side HTC is the quadratic mean of the inner and the overall HTCs, and is equal to 18, 17.2, 15.7, 19.9, 15.4% for the K11, K19, K26, K32 and K40 tubes, respectively.

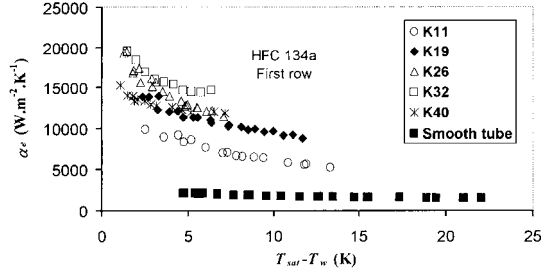


Fig. 3. Heat transfer coefficient on the first row during condensation of HFC 134a.

4. Experimental results and discussion

4.1. Behaviour of the pure fluid

Fig. 3 presents the evolution of the vapour-side HTC with temperature difference ΔT ($=T_{\text{sat}}-T_w$) during condensation of R134a, outside the first row of each tube. The figure shows the classical behaviour of the condensation HTC which decreases with increasing ΔT , that is, by increasing the thickness of the film condensate. This is the only significant thermal resistance on the vapour-side during condensation of pure fluids. For comparison, the HTC for a smooth tube [1] with a diameter identical to the fin root diameter is also shown. It can be seen that the heat transfer enhancement $\varepsilon_{\Delta T}$ is higher than the surface augmentation due to fins, because the surface tension forces drain condensate on the fin flanks and enhance the heat transfer. For example, for the K26 tube at $\Delta T=5$ K, due to surface tension forces, the heat transfer enhancement ratio is $\varepsilon_{\Delta T}=6$ for a surface augmentation of 4.4. Fig. 3 shows also that the HTC seems to reach an optimum for the K32 tube. Four models have been selected for comparison with experimental results, namely those proposed by Beatty and Katz [2], Rose [5], Murata and Hashizume [8], and Honda et al. [18]. Fig. 4 shows the influence of the fin pitch on the HTC during condensation of HFC134a, as predicted by these models and experimental data. Only the Rose's model can predict the optimum fin pitch within 0.65 mm, whereas the present experimental data show a fin

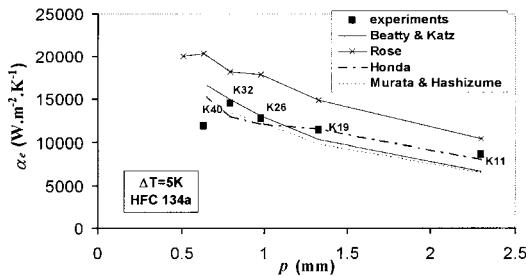


Fig. 4. Influence of the fin pitch on the heat transfer coefficient of a pure fluid. Comparison with models.

pitch optimum of 0.79 mm. It should be noted that the Honda's model can predict an optimum of the fin spacing as seen for other fluids (R113, ethylene glycol, steam) [18]. The Beatty and Katz model cannot in any way predict this optimum whatever the fluid tested because it does not take surface tension into account.

To get a good representation of the inundation effect in tube bundles, the ratio of the HTC of each row to that of the first row versus the row number is plotted in Fig. 5. It appears that the inundation effect is more important for tubes having large fin pitches (K11) where the ratio α_j/α_1 reaches 0.7 as for smooth tubes [1], whereas for tubes having low fin pitches (K32) the decrease in the HTC throughout the tube bundle is less than 10%. To predict the evolution of the HTC of each tube in a bundle is particularly difficult because of the unpredictable condensate flow pattern, combining both the effect of condensate inundation and the shear stress in the vapour.

Fig. 5 compares experimental HTC for each odd row with some available models. Two types of models have been chosen. The first one consists of an empirical correction given by Katz and Geist [19] to the Nusselt correlation developed for smooth tubes:

$$\frac{\alpha_j}{\alpha_1} = j^{1-\beta} - (j-1)^{1-\beta} \quad (4)$$

where j is the row number and α_j is the HTC of the j th row.

Nusselt has given a value of $1/4$ to β in smooth tube cases. However, Katz and Geist [19] found that the HTC deterioration for finned tube bundles is less important than for smooth tubes, so they proposed a value of 0.04 for β .

The second type of model is more rigorous and is represented by those of Honda et al. [18] and Murata and Hashizume [8]. They calculate the first row HTC as well as those of the other rows. Fig. 5 shows that the Honda et al. and Murata and Hashizume models predict very well the inundation effect for tubes having low fin pitch. The results of Katz and Geist correlation are comparable to those of Honda et al. and Murata and Hashizume in spite of its simplicity. Nevertheless, the Nusselt model developed initially for smooth tubes overestimates the inundation effect.

4.2. Behaviour of binary zeotropic mixtures

As noted previously, condensation of zeotropic mixtures is completely different from condensation of pure fluids because the condensation does not occur isothermally as with pure fluid condensation. Fig. 6 shows the influence of the more volatile component HFC 23 on the vapour side HTC α_e and it can be seen that the introduction of 6% of HFC 23 in the liquid phase (the equivalent of 18% of HFC 23 in the vapour phase at the

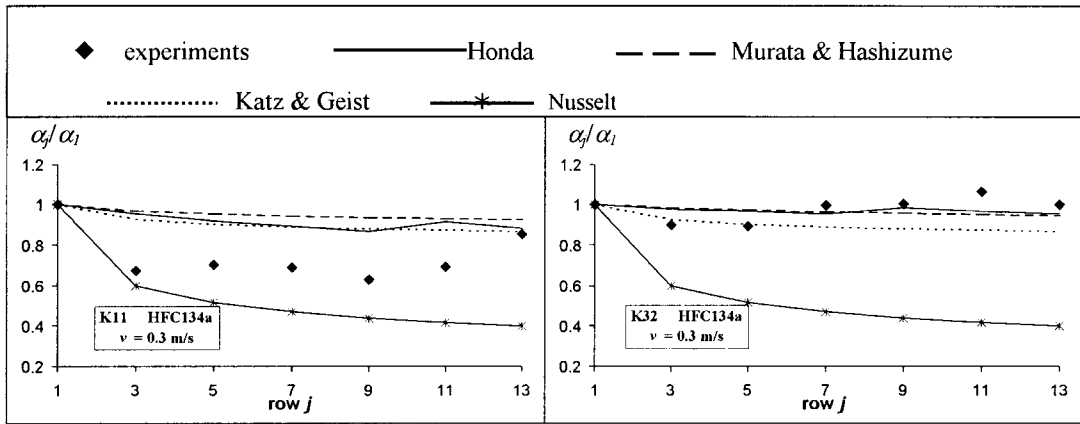


Fig. 5. Evolution of the HTC in the bundle. Comparison between experimental results and published models.

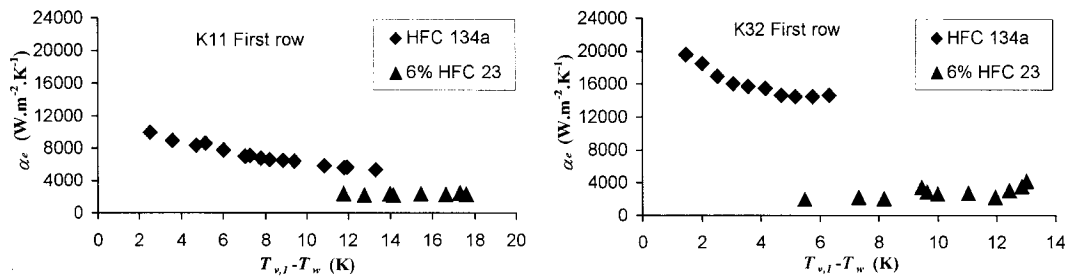


Fig. 6. Condensation of the HFC 23/HFC 134a mixture. Influence of the fin density on the HTC.

inlet of the test section), decreases considerably the HTC. This is due to an additional diffusion resistance which adds to the classical thermal resistance of the film condensate. This resistance comes from the diffusion layer, developed by the more volatile component (HFC 23) vapour, swept by the condensate rich in HFC134a toward the liquid-vapour interface. This deteriorates the HTC. Fig. 6 shows that the evolution of the HTC with ΔT is not the same for a pure fluid as for mixtures. In pure fluids, the thermal resistance between the vapour bulk and the wall is essentially due to the conduction resistance of the condensate film. In zeotropic mixtures, this thermal resistance is the sum of the condensate and the diffusion layer resistances. The condensate thermal resistance increases with ΔT whereas the diffusion layer resistance decreases. This decrease is probably due to increasing the vapour flow which could reduce the thickness of the diffusion layer. For smaller values of ΔT , the thermal resistance is controlled by the diffusion layer and the HTC increases. For higher values of ΔT it is controlled by the condensate layer. One can see that for HFC134a, the HTC decreases with increasing ΔT , since the thermal resistance is controlled by the condensate thickness. For zeotropic mixtures the HTC increases with ΔT , due to the diminution of the diffusion layer by condensation of the more volatile component when ΔT increases. The diffusion layer, which causes the deterioration of the

HTC, controls the heat transfer during condensation of zeotropic mixtures, and its diminution with increasing ΔT improves the HTC, even if the film condensate resistance due to its thickness is more important.

Fig. 6 shows also the influence of the tube type on the behaviour of the HTC as a function of ΔT for a given mixture composition (6% HFC 23). Compared to the pure fluid, it appears that the HTC coefficient deterioration is more important for tubes having a higher fin density. For $\Delta T = 7$ K, the K32 tube HTC is divided by a factor of 9, whereas for the K11 tube the HTC is divided by 2.5 for $\Delta T = 13$ K.

The inundation effect is not significant during condensation of zeotropic mixtures outside finned tube banks, since not only there is no deterioration of the

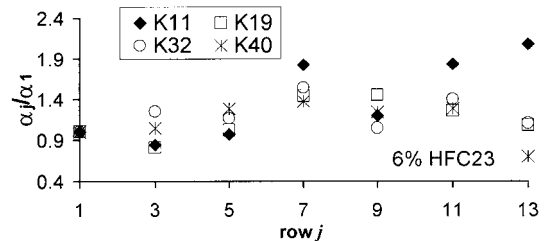


Fig. 7. Evolution of the HTC in the tube bundle during condensation of the HFC 23/HFC 134a mixture.

HTC in the tube bundle, but the HTC increases throughout (Fig. 7). It appears that the condensate flowing from the upper row disturbs the diffusion layer which basically leads to low HTCs in comparison with pure fluids, then the HTC increases in the bundle but not enough to reach pure fluids HTC values. The HTC augmentation is significant for mixtures rich in HFC 23, because the diffusion phenomenon is more important, and a small disturbance of the diffusion layer by the condensate flowing from the upper rows has a more significant impact than for a mixture poor in HFC 23.

5. Theoretical modelling

A way to model the HTC during condensation of zeotropic mixtures is to use the Bell and Ghaly method [20], which is based on the Silver model [21] developed to give an easy alternative to film theory judged to be complex for industrial modelling. The Bell and Ghaly model is based on the following hypotheses: the liquid and the vapour are in equilibrium at the bulk temperature, the condensate and vapour enthalpies are calculated at the bulk temperature, the sensible heat in the vapour phase is calculated using a single phase convective correlation. The Bell and Ghaly method does not require the determination of the liquid-vapour interface temperature. The condensation HTC α_e is calculated using:

$$\frac{1}{\alpha_e} = \frac{1}{\alpha_l} + \frac{Z}{\alpha_v} \quad (5)$$

The HTC of the condensate film α_l can be calculated by the Beatty and Katz model. To calculate the HTC α_e for each row (other than the first row) the Katz and Geist correlation [Eq. (4), with $\beta = 0.04$] is used. α_v is the HTC of the vapour phase, calculated as follows [22]:

$$\alpha_v = F \cdot \alpha_{\text{avg}} \quad (6)$$

F is a correction factor taking into account the fact that the vapour phase HTC of the upper rows in the bundle is less than the mean HTC of the bundle. F is equal to 0.7, 0.8, 0.87, 0.92 and 0.95, for the 1st, 2nd, 3rd, 4th and 5th rows, respectively, and to 1 for the 6th row and more. The mean HTC of the bundle in the gas phase is defined as:

$$\alpha_{\text{avg}} = \frac{Nu_v \lambda_v}{D_r} \quad (7)$$

Nu_v is the Nusselt number calculated by the expression [23]:

$$Nu_v = 0.29 \text{Re}_v^{0.633} \text{Pr}_v^{0.333} A^{-0.17} \quad (8)$$

A is the ratio of the total exchange surface area of the tube by the surface area of a plain tube with a diameter D_r .

The parameter Z is given by:

$$Z = x_g C_{p,g} \frac{dT}{dh_m} \quad (9)$$

x_g is the mass fraction of the vapour, $C_{p,g}$ the specific heat of gaseous mixture and dT/dh_m the slope of the equilibrium condensation curve $T=f(h_m)$, h_m being the specific enthalpy of the fluid.

As the lower part of the tube is flooded the heat transfer on the fins is not effective; to take into account the condensate retention in the lower part of the tubes, Eq. (8) is modified as follows:

$$\frac{1}{\alpha_e} = \frac{1}{\alpha_l} + \frac{Z}{\alpha_v \cdot A \cdot \Phi / \pi} \quad (10)$$

Φ is the flooding angle calculated by the Honda et al. equation [24]:

$$\Phi = \cos^{-1} \left(\frac{4}{\rho_l} \frac{\sigma \cos \theta}{g b D_e} - 1 \right) \quad (11)$$

The calculations are carried out as follows. The pressure P and temperature T at the inlet of the test section and the HFC 23 mass fraction in the liquid phase in the evaporator y_l (fixed by the operator) is used to calculate the HFC 23 vapour mass fraction y_v at the inlet of the test section. Given the heater power the refrigerant vapour flow rate in the trial loop is then calculated. With the flow rate and the inlet temperature of the water, the outlet temperature is derived.

The procedure calculation comprises the following steps:

- Step 1: calculate y_v (with refprop software [25]) from P , T and y_l .
- Step 2: calculate physical properties of the vapour at the inlet of the test section with respect to (y_v , P , T), and calculate dT/dh_m with Refprop. An integral condensation curve is assumed. For all rows flash calculations based on inlet composition are carried out.
- Step 3: calculate Z with Eq. (9) ($x_g = 1$ for the first row $j = 1$, and is calculated using the condensate flowrate for the other rows $j > 1$).
- Step 4: estimate ΔT .
- Step 5: calculate α_l using Beatty and Katz's model for $j = 1$, and combined with Katz and Geist's correlation [Eq. (4) with $\beta = 0.04$] for $j > 1$.
- Step 6: calculate α_v using Eqs. (6)–(8).
- Step 7: calculate α_e with Eq. 10, and calculate the heat flux Q_1 given by:

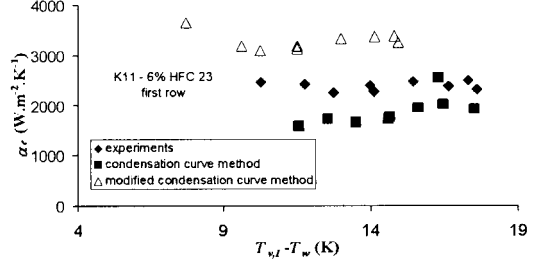
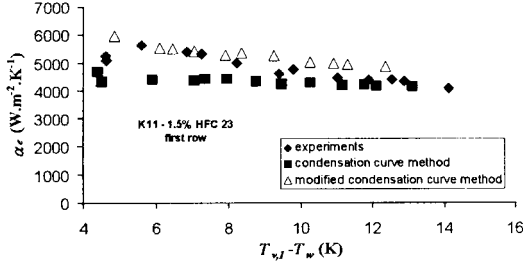


Fig. 8. Comparison between experimental results and the condensation curve method during condensation of HFC 23/HFC 134a on the first row.

$$Q_1 = \alpha_c S_r (T_{v,j} - T_w) \quad (12)$$

$T_{v,j}$ is the vapour temperature in the neighbourhood of the j th row.

- Step 8: calculate the outlet water temperature $T_{c,out}$ using Q_1 and the water flow rate.
- Step 9: calculate α_i using Eq. (3), and calculate the heat flux Q_2 given by:

$$Q_2 = \alpha_i S_i (T_w - (T_{c,in} + T_{c,out})/2) \quad (13)$$

- Step 10: compare Q_1 and Q_2 . If they are not equal go to step 4, if they are equal calculate the vapour temperature $T_{v,j+1}$ in the neighbourhood of the $(j+1)$ th row, with:

$$Q_2 = Q_1 = \dot{m}_v C_{p,v} (T_{v,j} - T_{v,j+1}) \quad (14)$$

- Step 11: calculate the vapour composition with the new vapour inlet temperature $T_{v,j+1}$, with pressure assumed to be constant in the test section.
- Step 12: go to step 2.

6. Comparison between experimental data and theoretical results

Fig. 8 compares the equilibrium method calculations and experimental results. It appears clearly that the equilibrium method (condensation curve method) underestimates experimental data. The underestimation means that the equilibrium method gives more importance to the diffusion phenomenon. The explanation for this is an overestimation of the factor Z in Eq. (5). Indeed, the factor Z is, ratio of the gas-side to total heat fluxes, is determined by Eq. (9). The gas-side heat flux is calculated without taking into account the mass transfer, which acts in the adverse sense of the heat flow. In this way the gas side heat flux is overestimated

and so is the factor Z . The Lewis number is the more appropriate dimensionless number for taking into account the relative contribution of heat transfer and mass transfer:

$$Le = \frac{a}{D_{1,2}} \quad (15)$$

a is the thermal diffusivity and $D_{1,2}$ is the binary diffusion coefficient [26].

Webb et al. [27] noted that equilibrium method shows errors of -50 or $+100\%$ with fluids having a Lewis number less than 0.6 or greater than 1 , respectively. Compositions tested in this work have a Lewis number ranging between 0.45 and 0.5 .

Correction to the condensation curve method can be achieved by the introduction of the Lewis number in the formulation of the Z factor thus:

$$Z \bullet = \frac{q_g}{q_T} = x_g C_{p,g} \frac{dT}{dh_m} Le^\gamma \quad (16)$$

Fig. 8 (modified condensation curve method) shows the amelioration given by this correction (with $\gamma = 3/2$, which is the value previously used in the case of smooth tubes [1]). It is clear that the results are improved upon in comparison with the classical equilibrium method, but overestimate slightly the experimental results. Calculations show that this overestimation is more pro-

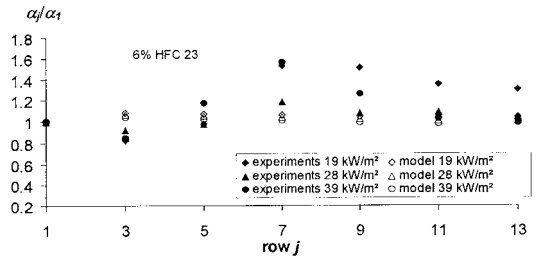


Fig. 9. Evolution of the measured and the calculated local HTC's in the tube bundle during condensation of a zeotropic mixture in a bundle of K19 tubes.

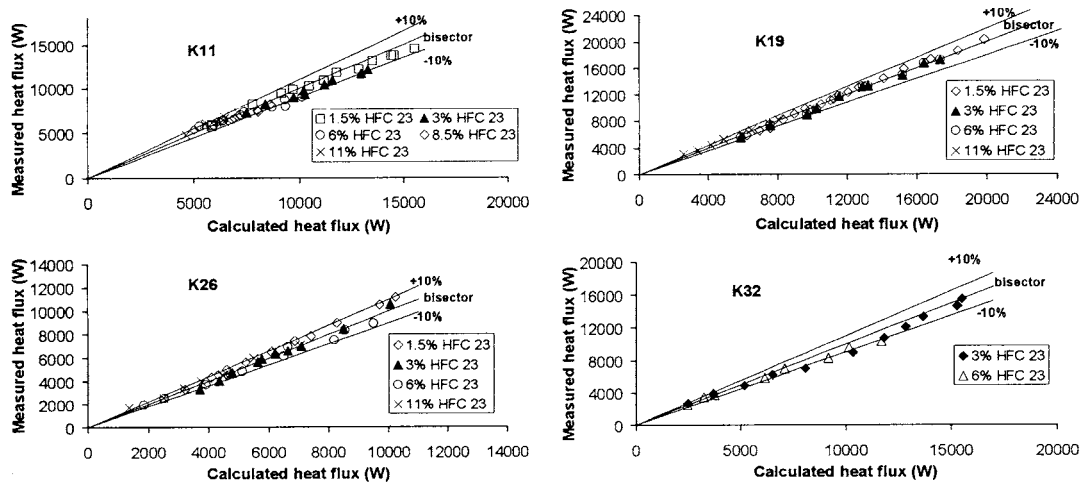


Fig. 10. Comparison of the measured and calculated heat fluxes during condensation of HFC 23/HFC 134a.

nounced for K19, K26 and K32, whilst, the classical equilibrium method underestimates always the experimental results. It can be noted that for all tested tubes, the constant γ value is insufficient to predict the HTC successfully, even if $\gamma = 3/2$ gives very good results in the case of smooth tubes [1].

Fig. 9 compares the calculated and the measured values of the ratio α_j/α_1 plotted versus the row number j using the modified condensation curve method, during condensation of several compositions of the HFC 23/HFC 134a mixture outside a bundle of K19 tubes. The model does not predict the strong increase in the HTC between the 3rd and the 7th row shown by the experimental results. Such behaviour could be expected since the model does not take into account either the disturbances of the gas diffusion layer by the condensate falling from the upper rows, or the vapour shear stress responsible of the increase in HTC in the bundle during condensation of zeotropic mixtures.

From an industrial point of view, the sizing of condensers requires the determination of the total exchanged heat flux. Fig. 10 compares the heat fluxes measured and calculated by the model during condensation of different compositions of the zeotropic mixture HFC 23/HFC 134a on the K11, K19, K26, K32 and K40 tube bundles. The predictive model and test results agree to within $\pm 10\%$. Consequently, even if the modified condensation curve method does not accurately predict the local HTC in the tube bundle during condensation of zeotropic mixtures, it gives good results when used to calculate the total heat flux.

7. Conclusions

Film condensation of downward flowing vapour on staggered bundles of horizontal finned tubes, using the

HFC 134a and the binary zeotropic mixture HFC 23/HFC 134a, was experimentally investigated using five commercial tubes with different fin pitches. The conclusions are as follows:

1. The optimal fin pitch during condensation of HFC 134a was found to be 32 fins/inch corresponding to the K32 tube.
2. The inundation effect is more important for tubes having large fin pitches. The Honda et al., Murata and Hashizume, and Katz and Geist models predict the HTC behaviour in the tube bundle reasonably well.
3. The HTC decreases dramatically compared to R134a when using the zeotropic mixture R23/R134a.
4. During condensation of the HFC 23/HFC 134a mixture, the HTC increases on the first rows ($j \leq 7$) because the diffusion layer is disturbed by the condensate flowing from the upper rows.
5. The condensate curve method underestimates the HTC on the first row. The modified condensation curve proposed predicts to within $\pm 10\%$ the heat flux of the whole condenser, but does not accurately predict the local HTC on each row.

References

- [1] Belghazi M, Bontemps A, Signe JC, Marvillet C. Condensation heat transfer of a pure fluid and binary mixture outside a bundle of smooth horizontal tubes. Comparison of experimental results and a classical model. *Int J Refrigeration* 2001;24:841–55.
- [2] Beatty KO, Katz DL. Condensation of vapors on outside of finned tubes. *Chemical Engineering Progress* 1948;44:55–77.
- [3] Gregorig R. Film condensation on finely rippled surfaces with consideration of surface tension. *Z Angew Math Phys* 1954;5:36–49.

- [4] Shah RK, Zhou SQ, Tagavi KA. The role of surface tension in film condensation in extended surface passages. *J Enhanced Heat Transfer* 1999;6:179–216.
- [5] Rose JW. An approximate equation for the vapour-side heat-transfer coefficient for condensation on low-finned tubes. *Int J Heat and Mass Transfer* 1994;37:865–75.
- [6] Honda H, Nozu S. A prediction method for heat transfer during film condensation on horizontal low integral-fin tubes. *Trans ASME, J Heat Transfer* 1987;109:218–25.
- [7] Honda H, Nozu S, Takeda Y. A theoretical model of film condensation in bundle of horizontal low finned tubes. *ASME, J of Heat Transfer* 1989;111:525–32.
- [8] Murata K, Hashizume CG. Prediction of condensation heat transfer coefficient in horizontal integral-fin tube bundles. *Experimental Heat Transfer* 1992;5:115–30.
- [9] Blanc P. Condensation des fluides frigorigènes HFC134a HCFC22 à l'extérieur d'un faisceau de tubes horizontaux améliorés. Thèse de doctorat, Université Joseph Fourier, Grenoble, France, 1994.
- [10] Honda H, Takamatsu H, Takada N, Yamasaki T. Condensation of HFC-134a and HCFC-123 in a staggered bundle of horizontal finned tubes. In: *Eurotherm 47, Heat Transfer in Condensation*, Grenoble, 4–5 October 1995. p. 110–5.
- [11] Cheng WY, Wang C. Condensation of R-134a on enhanced tubes. *ASHRAE Trans. Sympos., OR-94-10-1*, 1994. p. 809–17.
- [12] Ravi K, Varma HK, Mohanty B, Agrawal KN. Condensation of R-134a vapor over single horizontal circular integral-fin tubes with trapezoidal fins. *Heat Transfer Engineering* 2000;21:29–39.
- [13] Hijikata K, Himeno N. Condensation of azeotropic and nonazeotropic binary vapor mixtures. In: *Annual review of heat transfer*, Vol. 3, 1990. p. 39–83 [Chapter 2].
- [14] Honda H, Takuma M, Takada N. Condensation of downward-flowing zeotropic mixture HFC-123/HFC-134a on a staggered bundle of horizontal low-finned tubes. *J Heat Transfer* 1999;121:405–12.
- [15] Gnielinski V. New equation for heat and mass transfer in turbulent pipe and channel flow. *Int Chem Eng* 1976;16:359–68.
- [16] Khartabil HF, Christensen RN, Richards DE. A modified Wilson plot technique for determining heat transfer correlations. *Proc Second UK Natl Conf on Heat Transfer* 1988;II:1331–57.
- [17] Moffat RJ. Describing the uncertainties in experimental results. *Exp Thermal Fluid Sci* 1988;1:3–17.
- [18] Honda H, Nozu S. A generalized prediction method for heat transfer during film condensation on horizontal low finned tube. *ASME-JSME Thermal Eng Conf* 1987;4:385–92.
- [19] Katz DL, Geist JM. Condensation of six finned tubes in a vertical row. *Trans ASME, J Heat Transfer* 1948;70:907–14.
- [20] Bell KJ, Ghaly MA. An approximate generalized design method for multicomponent/partial condensers. *Trans ASME* 1973;69:72–9.
- [21] Silver L. Gas cooling with aqueous condensation. *Trans Inst Chem Eng* 1947;25:30–42.
- [22] Stasiulevicius J, Skrinska A. Heat transfer of finned tube bundles in crossflow. Hemisphere Publishing Corporation, 1987.
- [23] P.F.R. Engineering Systems. Heat transfer and pressure drop characteristics of dry towers extended surfaces. BNWL-PFR-7-102, INC.. Marina del Rey (CA, USA): PFR Inc; 1976.
- [24] Honda H, Nozu S, Mitsumori K. Augmentation of condensation on horizontal finned tubes attaching a porous drainage plate. *ASME-JSME Thermal Eng Joint Conf* 1983;3:289–96.
- [25] Gallagher J, McLinden M, Morrison G, Huber M. Software REFPROP, NIST thermodynamic properties of refrigerants and refrigerant mixtures database, Version 5.0, 1993.
- [26] Guide technique de THERMIQUE Dunod, 1981.
- [27] Webb DR, Fahrner M, Schwaab R. The relationship between the Colburn and Silver methods of condenser design. *Int J Heat Mass Transfer* 1996;39:3147–56.